



# Interaction of gabaergic ketones with model membranes: A molecular dynamics and experimental approach

Virginia Miguel, Mariela E. Sánchez-Borzzone, Daniel A. García\*

Universidad Nacional de Córdoba, Facultad de Ciencias Exactas, Físicas y Naturales, Departamento de Química, Cátedra de Química Biológica, Córdoba, Argentina  
Instituto de Investigaciones Biológicas y Tecnológicas (IIBYT), CONICET-Universidad Nacional de Córdoba, Córdoba, Argentina

## ARTICLE INFO

### Keywords:

Gabaergic ketones  
Mentha  
Insecticide  
Membrane interaction  
Molecular dynamic simulations  
Membrane fluidity

## ABSTRACT

$\gamma$ -Aminobutyric-acid receptor (GABA<sub>A</sub>-R), a membrane intrinsic protein, is activated by GABA and modulated by a wide variety of recognized drugs. GABA<sub>A</sub>-R is also target for several insecticides which act by recognition of a non-competitive blocking site. *Mentha* oil is rich in several ketones with established activity against various insects/pests. Considering that mint ketones are highly lipophilic, their action mechanism could involve, at least in part, a non-specific receptor modulation by interacting with the surrounding lipids. In the present work, we studied in detail the effect on membranes of five cyclic ketones present in mint plants, with demonstrated insecticide and gabaergic activity. Particularly, we have explored their effect on the organization and dynamics of the membrane, by using Molecular Dynamics (MD) Simulation studies in a bilayer model of DPPC. We performed free diffusion MD and obtained spatially resolved free energy profiles of ketones partition into bilayers based on umbrella sampling. The most favored location of ketones in the membrane corresponded to the lower region of the carbonyl groups. Both hydrocarbon chains were slightly affected by the presence of ketones, presenting an ordering effect for the methylene groups closer to the carbonyl. MD simulations results were also contrasted with experimental data from fluorescence anisotropy studies which evaluate changes in membrane fluidity. In agreement, these assays indicated that the presence of ketones between lipid molecules induced an enhancement of the intermolecular interaction, increasing the molecular order throughout the bilayer thickness.

## 1. Introduction

$\gamma$ -Aminobutyric acid (GABA) is the major inhibitory neurotransmitter in the vertebrate and invertebrate nervous system [1]. GABA<sub>A</sub> receptors (GABA<sub>A</sub>-R) are activated by GABA and their agonists, and modulated by a wide variety of recognized drugs, including barbiturates, anesthetics, and benzodiazepines [2]. GABA<sub>A</sub>-Rs are also targets for several insecticides and other toxicants which act by recognition of the picrotoxinin or noncompetitive antagonist site to block the receptor [3].

The genus *Mentha*, one of most the important members of the *Lamiaceae* family, is represented by many species commonly identified as mint, which have been known for its medicinal and aromatherapy properties. The insecticidal activity of *Mentha* oil and its main components has been tested and established against various insects/pests [4]. *Mentha* oil is rich in several monocyclic monoterpenes such as carvone, menthone, pulegone and dihydrocarvone [4]. Carvone, a natural terpene which can be purified as R(-) or S(+) enantiomers, has demonstrated insecticidal activity which may be explained by its

interaction with the GABA<sub>A</sub>-R at its non-competitive blocking site [5]. Moreover, we have recently reported that menthone, pulegone and dihydrocarvone are able to behave as GABA<sub>A</sub>-R negative allosteric modulators, at least in mammalian cells [6]. As a comparison, thujone, another cyclic ketone component of wormwood oil and some other herbal medicines, not only has demonstrated insecticidal activity, but also it has been described as a potent convulsant compound acting mainly at the noncompetitive blocker site of the GABA<sub>A</sub>-R [7,8].

However, even though GABA<sub>A</sub>-R function can be analyzed using well-described theories of ligand–receptor interactions, it should be considered that many compounds that regulate GABA<sub>A</sub>-R function are noticeably lipophilic (e.g., benzodiazepines, barbiturates, long-chain alcohols, and anesthetics), which may change the physical properties of the lipid bilayer. Thus, it is possible that the activity of lipophilic ketones on the receptor, as was previously mentioned, could be the combined result of the interaction of ketone molecules with specific receptor proteins (GABA<sub>A</sub>-R) and with the surrounding lipid molecules modulating the supramolecular organization of the receptor environment. [9–15]. Thus, more studies are required about the activities and

\* Corresponding author at: Instituto de Investigaciones Biológicas y Tecnológicas (IIBYT), CONICET-Universidad Nacional de Córdoba, Av. Vélez Sarsfield 1611, Córdoba 5016, Argentina.

E-mail address: [dagarcia@unc.edu.ar](mailto:dagarcia@unc.edu.ar) (D.A. García).

<https://doi.org/10.1016/j.bbamem.2018.05.012>

Received 2 January 2018; Received in revised form 23 May 2018; Accepted 24 May 2018

Available online 25 May 2018

0005-2736/ © 2018 Elsevier B.V. All rights reserved.

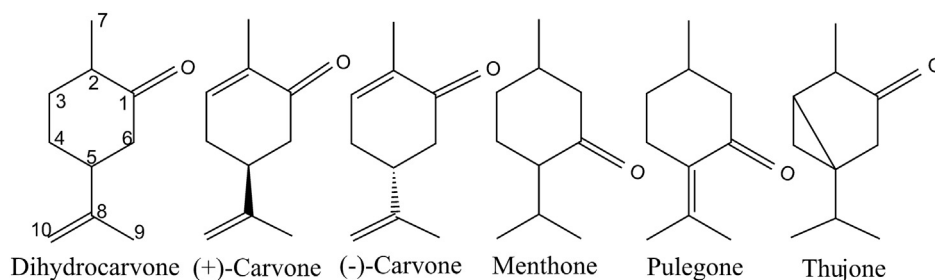


Fig. 1. Chemical structures of the compounds analyzed. The numbers in the dihydrocarvone graph represent the position of carbons.

molecular mechanisms responsible for the activity of some lipophilic compounds, which may be potential insecticides. Perturbation of physical membrane properties could be, at least in part, one of their modes of actions, as was suggested for some antimicrobial agents [16,17] and anesthetics [18].

Considering that mint ketones above detailed are highly lipophilic, it is expected they affect membrane properties. We have previously found, using lipidic monomolecular layers as an artificial model membrane, that dihydrocarvone and thujone can incorporate into a phospholipid monolayer reducing molecular repulsion among phospholipid headgroups [11]. Thujone, another cyclic ketone, possess similarities at molecular structure level with the selected mint compounds. While thujone presents a central bicyclic ring structure with six carbon atoms, mint ketones exhibit a cyclohexene (+ and – carvone) or cyclohexane (dihydrocarvone, menthone and pulegone) with comparable substituents to thujone (Fig. 1). The inclusion of this structurally similar compound, as a reference agent acting on the GABA<sub>A</sub>-R, will allow gaining insight into their effects on membranes, as part of the mechanism of action involved in receptor modulation.

In this article, we have explored the effect of five cyclic ketones, present in mint plants with demonstrated insecticide activity, on the organization and dynamics of the membrane, by using Molecular Dynamics (MD) Simulation studies in a bilayer model of 1,2-dipalmitoyl-*sn*-glycero-3-phosphocholine (DPPC). We performed free diffusion MD and obtained spatially resolved free energy profiles of ketones partition into DPPC bilayers based on umbrella sampling. MD simulations results were also contrasted with experimental data from fluorescence anisotropy studies which evaluate changes in membrane fluidity.

## 2. Materials and methods

### 2.1. Materials

*R*-(–) and *S*-(+)-carvone (5-isopropenyl-2-methyl-2-cyclohexen-1-one; purity > 98%), (*R*)-(+)-Pulegone((5*R*)-5-methyl-2-propan-2-ylidene-cyclohexan-1-one, purity 99%), (–)-menthone((2*S*,5*R*)-5-methyl-2-propan-2-ylcyclohexan-1-one, purity 99%), (+)-dihydrocarvone (2-methyl-5-prop-1-en-2-ylcyclohexan-1-one, ~77% *n*- (+)dihydrocarvone and ~20% iso-(+)dihydrocarvone), thujone (1-isopropyl-4-methylbicyclo[3.1.0]hexan-3-one; ~70%  $\alpha$  and ~10%  $\beta$ ) and DPH (1,6-diphenyl-1,3,5-hexatriene) were obtained from Sigma-Aldrich Chem (St. Louis, MO; USA). 1-2-Dipalmitoyl-*sn*-glycero-3-phosphocholine (DPPC) lipid was purchased from Avanti Polar Lipids (Alabaster, AL, USA). All other reagents were of the highest analytical grade. Solutions were prepared with double-deionized water.

### 2.2. Computational details

All simulations were carried out using the 4.6.3 GROMACS package with GPU acceleration [19]. The All Atom (AA) SLipids force field (FF) was used for lipids [20] and the TIP3P model [21] for water molecules. The starting geometries were obtained from SLipids on line resource

(<http://www.fos.su.se/~sasha/SLipids/Downloads.html>). Fully hydrated lipid bilayers (equilibrated at the mentioned temperatures) containing 128 1-2-dipalmitoyl-*sn*-glycero-3-phosphocholine (DPPC) molecules were employed for equilibrium simulations.

The construction of ketones units to be used in MD simulations was as before [22,23]. They were obtained with the antechamber module, using the GAFF force field, [24] employing the restricted ESP (RESP) charges obtained from a single point HF/6-31G\* [25,26] quantum chemical calculation of the optimized structure (at B3LYP/6-31 + G\* level) within the Gaussian 03 package [27]. The AnteChamber Python Parser interface (ACPYPE) [28] was employed to change the format of the parameter files in order to use them with GROMACS code. The Potential of Mean Force (PMF) simulations were carried out in a fully hydrated lipid DPPC bilayer containing 64 lipid molecules. Free energy profile results were derived from the PMF  $\Delta G(z)$  calculation as a function of the distance of the ketones to the bilayer center along the *z*-axis normal to the plane of the bilayer. A series of 20 separate simulations, of 30 ns each, were performed, in which each molecule was restrained to a given depth in the bilayer by a harmonic restraint on the *z*-coordinate. A force constant of 1000 kJ/mol nm<sup>-2</sup> was used with a spacing of 0.2 nm between the centers of the biasing potentials. Two ketones molecules were used, one per leaflet allowing error estimation. Finally, the Weighted Histogram Analysis Method (WHAM) was used to extract the PMF and calculate  $\Delta G$  [29]. The error bars for these calculations were obtained using the bootstrap method [30].

For free diffusion MD, the simulation protocols were the same as in reference [20]. For each ketone, 20 molecules were randomly located in the water solvent within the simulation boxes with the following dimensions in the *x*-*y*-*z* axes, ~68 Å × ~68 Å × ~74 Å. We used the MD parameters available in the Stockholm lipids home page (<http://www.fos.su.se/~sasha/SLipids/Downloads.html>). All bonds were constrained using Lincs algorithm. Constraining the bond lengths allowed a time step of 2 fs to be used. The Lennard-Jones (LJ) interactions were truncated at 1.0 nm. The particle mesh Ewald method [31] was used to evaluate the electrostatic interactions, with a cutoff of 1.0 nm. The simulations were performed at an NPT ensemble. ~250 ns of MD simulations at 50 °C (323 K) within the NPT ensemble were collected for all the systems, the final 150 ns of these simulations were employed for the analysis of density profiles, deuterium order parameter, etc.

### 2.3. Experimental assay

#### 2.3.1. Preparation of large unilamellar vesicles

Multilamellar large vesicles (MLVs) were prepared as described elsewhere [32]. The appropriate amount of DPPC dissolved in chloroform was placed in a glass tube and evaporated under a stream of nitrogen with constant rotation to facilitate the formation of a thin lipid film; traces of solvent were removed under vacuum. The dried lipid was suspended in water at a final concentration of 41  $\mu$ M (0.03 mg/ml) by repeating seven consecutive cycles of heating at 65 °C for 1 min plus vortexing for 30 s, and MLVs were formed. Large unilamellar vesicles (LUVs) of homogeneous size were obtained by extruding 19 times the MLVs suspension through 100-nm pore size Whatman polycarbonate

filters using a mini extruder Liposofast (Avestin, Canada).

### 2.3.2. Fluorescence anisotropy

The fluorescent probe DPH (0.82  $\mu\text{M}$ ) was added to the DPPC-LUV suspension (prepared as described above) and incubated for 1 h at 50 °C. The effect of different ketones (1 mM) on DPH steady-state fluorescence anisotropy was studied. LUVs samples were incubated for 30 min after the addition of the ketones. The first recording was taken at 50 °C and then the temperature was lowered to 40 ° and 25 °C allowing stabilization of the sample for 10 min in each case.

Anisotropy values were calculated from the emission fluorescence intensities at  $\lambda_{\text{em}} = 430 \text{ nm}$  ( $\lambda_{\text{ex}} = 356 \text{ nm}$ ) measured with the excitation, and the sample polarizer filters oriented parallel and perpendicularly one with respect to the other, in a L-format FluoroMax-3 spectrofluorometer (JovinYvon, Horiba). Slits width and integration time were set at 2 nm and 1 s, respectively. Control samples containing DMSO were tested to rule out the effect of this solvent.

Steady-state fluorescence anisotropy (FA) was calculated using Eq. (1):

$$FA = \frac{I_{VV} - I_{VH} \cdot G}{I_{VV} + 2 \cdot I_{VH} \cdot G} \quad G = \frac{I_{HV}}{I_{HH}} \quad (1)$$

where  $I_{VV}$ ,  $I_{HH}$ ,  $I_{VH}$ , and  $I_{HV}$  are the values of the different measurements of fluorescence intensity taken with both polarizers in vertical (VV) and horizontal (HH) orientations or with the excitation polarizer vertical and the emission polarizer horizontal (VH) or vice versa (HV).  $G$  is a correction factor for differences in sensitivity of the detection system for vertically and horizontally polarized light [32].

## 3. Results and discussion

In the present study, we evaluate the membrane interaction of five cyclic ketones present in mint plants, with proved insecticide/larvicide effects and gabaergic activity, including other known gabaergic ketone used as reference compound (thujone) [3–6]. The work involves MD simulations of their partition into the bilayer as well as a fluorescence anisotropy study as experimental approach. MD simulations have been widely used to study drug-membrane systems to capture the interaction details on the molecular level, that could be comparable to complementary experimental methodologies [33].

### 3.1. All atom equilibrium MD simulations

In order to study and to describe the interaction of the different ketones with the DPPC membrane, MD runs of  $\sim 250 \text{ ns}$  each were carried out with 20 molecules located at random starting positions within 5 to 25 Å over the membrane plane. With the purpose of corroborating the proper equilibration of MD simulations, the area per lipid and membrane thickness were also evaluated (see Table S1).

Fig. 2 shows the density profile during the last 150 ns simulation along the normal to the membrane plane ( $z$  axis) of different DPPC membrane components, as well as ketones molecules. The peak of ketones density in the membrane is found in the lower region of the carbonyl groups of DPPC indicating their preferential location in the bilayer. The degree of ordering of the acyl chains of the phospholipids, the deuterium order parameter  $S_{\text{CD}}$  [34], was employed to evaluate the effect of the interaction of ketones with the membrane in the acyl chain region. Fig. 3 shows a comparison of the  $S_{\text{CD}}$  values of  $sn1$  and  $sn2$  chains of a DPPC bilayer at fluid phase (50 °C) compared to  $S_{\text{CD}}$  values of both chains of a DPPC bilayer in presence of the different ketones. It was found that both  $sn1$  and  $sn2$  chains were slightly affected by the presence of all compounds, presenting an ordering effect for the methylene groups closer to the carbonyl (Fig. 3). This is in agreement with the preferred location of ketones inside the bilayer according to density profiles (Fig. 2). The rigidity and high ordering of the glycerol backbone region, establishing empty spaces below that zone, could also favor this

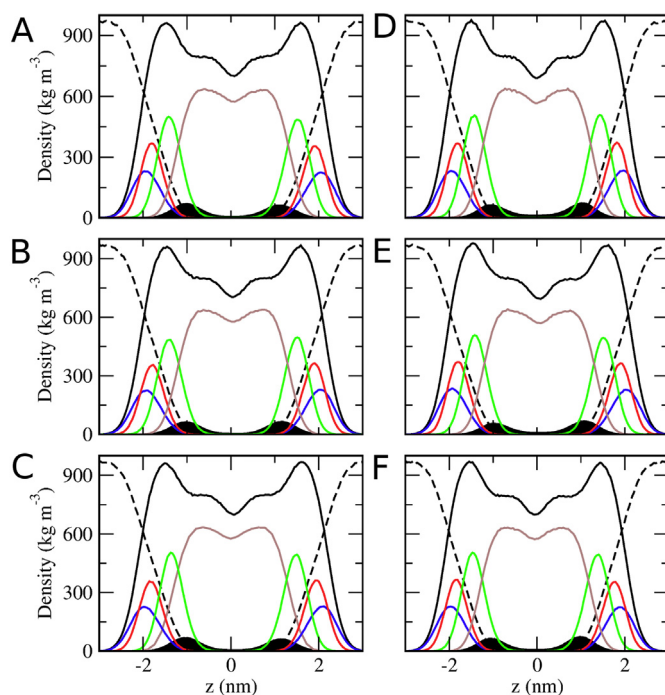


**Fig. 2.** Schematic diagrams of the density profile of DPPC bilayers in presence of different ketones along the  $z$ -axis. The density profile of the whole system and relevant components of the system are shown. Density profile of DPPC (black line), water (black dashed line), DPPC choline group (blue line), DPPC phosphate group (red line), DPPC carboxylic group (green line), DPPC acyl chain (brown line). A-Dihydrocarvone, B-(+)-Carvone, C-(-)-Carvone, D-Menthone, E-Pulegone and F-Thujone. All ketones are indicated with filled to zero black line.

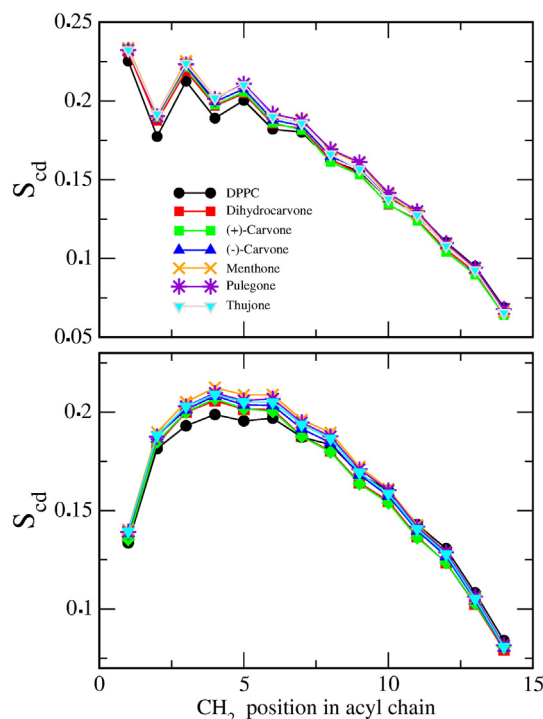


**Fig. 3.** Ketone effect on the deuterium order parameters ( $S_{\text{CD}}$ ) of DPPC acyl chains.  $S_{\text{CD}}$  values from  $sn1$  chain (upper panel) or  $sn2$  chain (lower panel) of DPPC bilayer were determined in absence or presence of ketones.

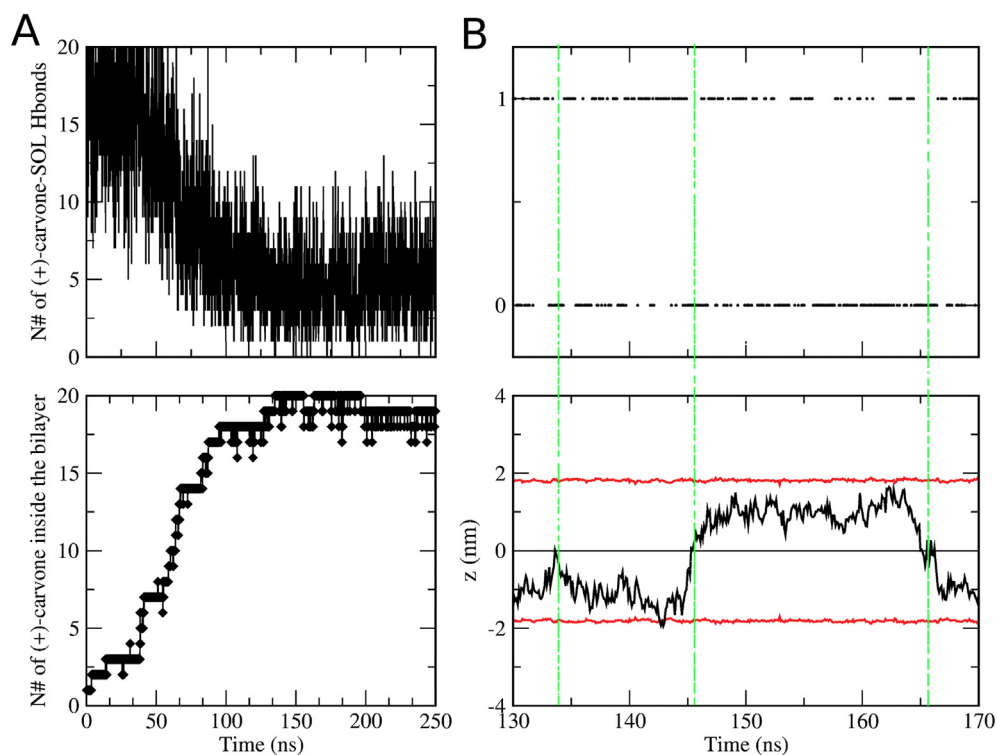


**Fig. 4.** Time evolution of hydrogen bonds of a reference ketone. A-Total number of hydrogen bonds of (+)-carvone molecules with water during free diffusion MD (upper panel-black line) compared to the number of molecules inside the bilayer (lower panel-black line and diamond symbol). B- Hydrogen bonds of a single (+)-carvone molecule (upper panel-black line) and its position along the z axis (lower panel-black line; in red line the position of lipid head-groups). (+)-Carvone translocations from one hemilayer to the other are indicated (green punctuated lines).

ketone location [35,36].

The diffusion of ketones inside the bilayer was assessed along the MD. All ketones molecules were found inside the bilayer at 125 ns (Fig. S2). Following the exact position of all ketones in the z axis (Fig. S1), it can be observed that most of the time the ketone molecule is inside the bilayer between the charged headgroups, while hemilayer translocation is a usual event.

We also estimated the water  $\rightarrow$  core free energies of partition from the unbiased simulations (Fig. 2). We estimated the partition coefficient as the coefficient of ketones partial density at the lipid phase and at the aqueous phase, using the data obtained in Fig. 2, and these values were used to calculate the  $\Delta G$  of partition [37]. The free energy values obtained were: dihydrocarvone:  $-12.93 \text{ kJ.mol}^{-1}$ , (+)-Carvone:  $-10.3 \text{ kJ.mol}^{-1}$ , (-)-Carvone:  $-12.37 \text{ kJ.mol}^{-1}$ , Menthone:  $-22.98 \text{ kJ.mol}^{-1}$ , Pulegone:  $-8.72 \text{ kJ.mol}^{-1}$  and Thujone:  $-12.93 \text{ kJ.mol}^{-1}$ .

In other computational analysis, we studied the time evolution of hydrogen bonds of ketones, both with water as well as with DPPC. When the total number of hydrogen bonds of ketones molecules with water was analyzed, a reduction associated with ketones insertion into the bilayer was observed (Fig. 4A). Water establishes hydrogen bonds as a donor being the carbonyl oxygen of the ketone its acceptor group. We followed the hydrogen bonds of each ketone molecule with water during a lapse time, when the compound resides within the bilayer and translocate through the membrane (see (+)-carvone as an example, Fig. 4B). It can be observed that when crossing the bilayer, ketone molecules are dehydrated (in Fig. 4B crosses events are indicated). Eventually, they can establish a hydrogen bond with a water molecule in the other hemilayer. Also, we determined the first hydration shell for (+)-carvone along the MD using *g\_trjorder* and a radius cut-off of 0.435 nm. While in the aqueous phase (+)-carvone has  $\sim 35$  water molecules, at the lipid phase there are  $\sim 5$  water molecules, except at translocations, were water molecules drop to zero (Fig. S3). Finally, we calculated the electrostatics (coulombic) and Van der Waals (LJ) interaction among water and ketones. A major reduction in attractive forces is observed for both types of non-bonding interaction (Fig. S4).

Finally, we analyzed the chemical groups that interact when ketones

enter to the bilayer, following the variation of the minimum distance among these groups (Fig. S5). This analysis showed that when ketones enter the bilayer, ketone-oxygen, carbon 7 (C7) and carbon 8 (C8) (see Fig. 1 for C positions) locate near the carboxyl group. Ketone-oxygen (O) also closely interacts with choline group (Fig. S5A). The distance between ketone-oxygen and carboxylic group was  $\sim 3.2 \text{ \AA}$ . The distance between ketone-oxygen and N of choline group was  $\sim 3.5 \text{ \AA}$ . The distance between ketones C7 and N of choline group was  $\sim 4.5 \text{ \AA}$ . Menthone and pulegone C7 are located at a slightly major distance than C7 of the rest of the ketones  $\sim 5 \text{ \AA}$ . The inverse situation is observed for C8 of both compounds when compared to the rest of the ketones (Fig. S5, B–C). Taking into account the minimum distances among atoms/chemical groups of both molecules, DPPC and ketone, the latter would locate with its ketone-oxygen oriented to DPPC polar head.

Further, we calculated the coulombic and LJ interaction among DPPC and ketones (Fig. S6). LJ interactions became more negative as ketones partition into the membrane and are, therefore a driving force of ketones partition into the membrane. It is expected that this interaction is with the DPPC hydrocarbonated chain.

### 3.2. PMF calculation of KETONES-DPPC interaction

We performed PMF calculations to determine the free energy profile of ketones partition at the bilayer. PMF were determined as a function of the distance to the center of the bilayer along its normal axis z [ $\Delta G(z)$ ]. Free energy profile calculations were derived from the PMF extracted from a series of umbrella sampling simulations. PMF calculation for each ketone was performed in a DPPC bilayer at liquid-crystalline state ( $50^\circ \text{C}$ ) (Fig. 5). PMF curves were aligned so that the ketones relative free energy in bulk water corresponds to zero in each case.

The shapes of the free energy profiles are similar for all ketones (Fig. 5B). There is a maximum in the charged head group region ( $\sim 2 \text{ nm}$  from the center of the bilayer) while the global minimum corresponds to the region of the carbonyl groups ( $\sim 1\text{--}1.5 \text{ nm}$ ). Thus, the most favored location of ketones in DPPC membrane would correspond to the interphase between the hydrophobic and the polar zone of



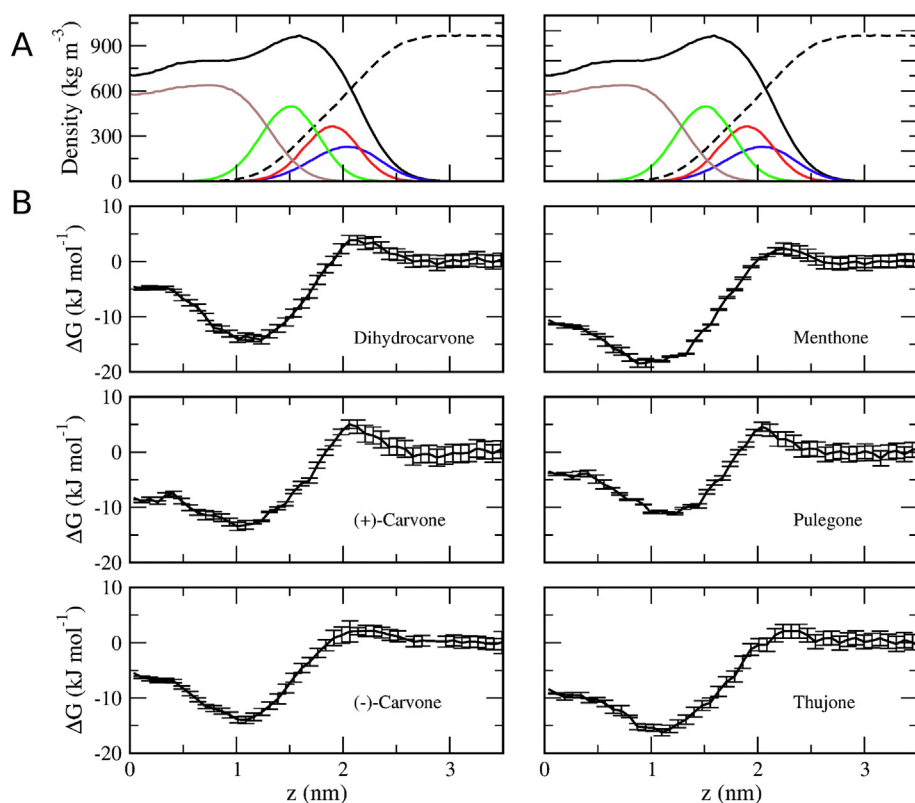


**Fig. 5.** PMF of Ketones free energy ( $\Delta G$ ) of partitioning into a DPPC bilayer. A-The two upper panels display the system partial densities: DPPC (black line), water (black punctuated line), DPPC choline group (blue line), DPPC phosphate group (red line), DPPC carboxylic group (green line), DPPC acyl chain (brown line). B-The six lower panels display each ketone free energy ( $\Delta G$ ) at 50 °C along the z axis.

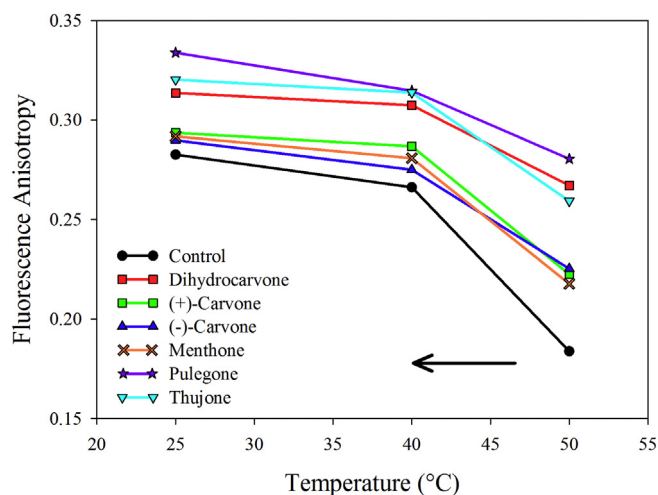


**Fig. 6.** Fluorescence anisotropy of DPH in DPPC LUVs at different temperatures in the presence of ketones (1 mM). The curves were performed reducing the temperature from 50 to 25 °C (as the arrow indicates).

the bilayer, being less probable their placement at the head group region. These results are in agreement with the maximum displayed by ketones density profile in unbiased MD simulations (see Fig. 2).

The calculated free energy change for transferring a ketone molecule from water to the bilayer center was approximate  $-5 \text{ kJ} \cdot \text{mol}^{-1}$  with an initial barrier of  $3 \text{ kJ} \cdot \text{mol}^{-1}$  for crossing the polar head of the bilayer and a minimum of  $-10$  to  $-20 \text{ kJ} \cdot \text{mol}^{-1}$ . In this sense, it is expected that all ketones can also translocate from one hemilayer of the membrane to the other, since their  $\Delta G$  have negative values at the bilayer center (0 nm) (Fig. 5B). These profiles are consistent with the maximum of density profiles in free diffusion MD simulations for ketones, that are located essentially in the DPPC carboxylic group region (Fig. 2).

We performed two additional PMF calculations using a different initial system setup. One system with two ketones molecules were one is biased from water to the bilayer core and the other one, in the aqueous phase, is free to diffuse and to interact with the biased molecule, and another system were two ketones molecules are biased from the bilayer core to water one per leaflet (Fig. S7). These results indicate that presence of a second molecule favored the partitions into the bilayer of dihydrocarvone, (+)-Carvone, (-)-Carvone and Thujone, while there was no effect on the partition of menthone and pulegone.

As mentioned above, we estimated the water  $\rightarrow$  core free energies of partition from the unbiased simulations (Fig. 2), where the free energy values obtained are consistent with the PMF profiles obtained in biased simulations, were menthone is the most lipophilic and pulegone the least.

### 3.3. Experimental analysis

Anisotropy values for DPH in DPPC LUVs were evaluated as a function of temperature (50–40–25 °C) in the presence of different ketones (1 mM).

In these experiments we used DPH due to its ability to localize through the hydrocarbon chain region of the bilayer and to sense monotonous changes in its microproperties modified by the temperature [38]. The temperature dependence of DPH fluorescence anisotropy on control samples containing DPPC (without any compound) showed an abrupt change near of 40 °C in agreement with the phase transition of DPPC [39] (Fig. 6). The complex structural dynamics of the bilayers is governed by temperature-dependent parameters such as the average interfacial area per lipid, thickness of bilayer, and disorder of hydrophobic tails, which determine their phase behavior. For saturated phosphatidylcholines, such as DPPC, the main transition between the liquid-crystalline phase and the gel phase (gel–fluid transition) occurs at 41.5 °C [39,40]. The results indicate that all compounds decreased the membrane fluidity at both, liquid-crystalline and gel bilayer phases. This effect indicates that the presence of ketones between lipid

molecules induces an enhancement of the intermolecular interaction, increasing the molecular order throughout the bilayer thickness, confirming their partition into the bilayer. Considering that the assays were performed from high to low temperatures, the ketones would be incorporated to the membrane in liquid-crystalline phase and maintained even at a stiffer gel phase. The decreased fluidity, induced by all ketones on DPPC bilayers, is in correspondence with the observed ordering effect described by the deuterium order parameter  $S_{CD}$  described above.

The election of DPH probe for the anisotropy assay is founded in its property to sense the hydrocarbon region where our theoretical calculus demonstrated ordering effects. The fluorescent probe TMA-DPH, with an additional charged group, is anchored at the lipid/water interface and reports on a bilayer region that is distinct from that of the hydrophobic DPH, which senses a deeper region [41]. However, employing atomistic MD simulations to characterize the behavior of DPH and TMA-DPH in 1-palmitoyl-2-oleoyl-*sn*-glycero-3-phosphocholine (POPC), Do Canto et al. [42] have demonstrated that the average location of TMA-DPH is only  $\sim 3\text{--}4$  Å more superficial than that of DPH. In that work, these authors described that both probes were able to induce a concentration-dependent alteration of  $S_{CD}$  values through the acyl chain. Consequently, it is expected that DPH behaves as an appropriated probe to sense the chain region where the simulation studies predict changes induced by ketones. In the present study, our computational results showed in Fig. 3, where all ketones were able to induce an ordering effect on the first atoms of the acyl chains, are in agreement with the rigidizing effect of these compounds experimentally demonstrated by fluorescence anisotropy using the DPH probe.

These computational studies can be contrasted with other previous experimental results obtained by our group. We have studied the membrane interactions of the ketones dihydrocarvone and thujone by using DPPC monolayers, which are widely applied to perform membrane interaction studies of lipophilic compounds. This approach allowed us to focus on the interaction between ketones and phospholipids, by recording molecular lateral pressure-area isotherms, including Brewster angle microscopy (BAM) of monolayers. These results support the hypothesis that the location of the ketone molecules reducing the repulsive forces among phospholipids headgroups allows a closer molecular packing, diminishing the mobility of the hydrocarbon chains [11], as was also described for gabaergic phenols [12,14]. This hypothesis is now totally in agreement with the present computational analysis, which confirm not only an interfacial location of ketone molecules in the bilayer, with strong influence on the headgroup region, but also a rigidizing/stiffening effect on the membrane core.

### 3.4. General remarks

There is a great demand to reduce the use of the synthetic pesticides and develop alternatives with fewer secondary effects on the environment and non-target organism. Natural products have long been used as pest controls for centuries, and in recent years they have become as the best alternatives to conventional pesticides [43]. Monoterpenoids, like the mint ketones assayed here, are one of the most successful botanical pesticide groups [4,44]. Since ketones are highly lipophilic compounds that present diverse effects difficult to explain only by specific protein binding/action, it is interesting to study their interactions with the lipid bilayer.

Lateral pressure profiles between lipid molecules have been suggested to play a significant role in the activation of membrane proteins through changes in their conformational state [18,45]. In this sense, we demonstrate that ketones here analyzed are lipophilic compounds that can penetrate DPPC lipid bilayers, producing alterations of the lateral organization. Furthermore, we have previously showed that the presence of ketones in the lipid interface induces a closer molecular packing in DPPC monolayers, diminishing the mobility of the hydrocarbon chains [11].

Small cyclic terpenes penetrate the membrane and interact with the glycerol backbone and phosphate groups of the lipid [12,14,33]. In agreement, all ketones here analyzed locate mainly to the region that comprehends the 1 to 1.2 nm from the bilayer center. This region corresponds to the interface between the lipid tails and the headgroups, since it represents: the peak of the lipid tail density, the bulk of the carbonyl density, a portion of the head group density and a small amount of water.

It has been previously showed that the introduction of a ketone group facilitates sterol flip-flop [46]. This result is in agreement with our observation that all ketones analyzed in this work were capable of trespassing one hemilayer to the other. It was suggested that ketone group can facilitate transmembrane mobility of steroid hormones, preventing them from a prolonged residence time in one of the membrane leaflets [46]. The flip-flop rates correlate inversely not only with the free energy penalty of carrying a more hydrophilic group across the membrane, but also with the strength of interactions between the lipid headgroups and the terpenes [47]. This may be a difference between ketones and alcohols, the later carrying a hydroxyl group that would difficult flip-flop movements.

Limonene and perillaldehyde are cyclic terpenes that have a common 4-isopropenyl-1-cyclohexene hydrophobic skeleton; perillaldehyde is more polar than limonene since the latter presents a ketone group. Limonene penetrated deepest into the hydrophobic core of the membrane, and a significant number of the molecules localized to the bilayer center [47]. This is agreement with our results, since ketones here analyzed present a similar partition to perillaldehyde.

Thymol, as well as other phenols structurally similar to propofol, have a rigid cyclic structure that locate in the region between the polar group (choline molecule), the glycerol and the first atoms of the acyl chains, close to the interfacial region. It has been observed that this location induced an increased order in the acyl chain close to the bilayer interface and a reduction in the molecular repulsion among phospholipid headgroups [14,48]. Similar molecular explanation would be suggested for ketone ordering effect.

## 4. Conclusions

In the present work, we study the membrane interaction of five cyclic ketones present in mint plants, including thujone as a reference compound, by using not only a theoretical-computational but also an experimental approach. The following main results were obtained:

- The most favored location of monoterpene ketones in DPPC membrane would correspond to the interphase between the hydrophobic and the polar zone of the bilayer, in the lower region of the carbonyl groups, being less probable their placement at the head group region.
- All ketones can translocate between both hemilayers of the DPPC bilayer as a usual event.
- Both hydrocarbon chains were slightly affected by the presence of ketones, presenting an ordering effect for the methylene groups closer to the carbonyl. In agreement, the experimental fluorescence results indicate that the presence of ketones between lipid molecules induces an enhancement of the intermolecular interaction, increasing the molecular order throughout the bilayer thickness.
- During their incorporation to the bilayer the ketones are dehydrated, as it was observed in the analysis of hydrogen bonds of ketone molecules with water

Considering their ability to interact and to change the physical properties of the lipid bilayer, it is possible to suppose that the mint ketones could modulate the supramolecular organization of biological membranes and consequently the membrane proteins functionality, contributing at least in part as the action mechanism which explains their insecticide bioactivity.

## Conflict of interest

The authors declare no conflicts of interest.

## Transparency document

The <http://dx.doi.org/10.1016/j.bbamem.2018.05.012> associated with this article can be found, in online version.

## Acknowledgements

The authors are grateful to SECyT-Universidad Nacional de Córdoba (Res. 313/16), FONCyT (PICT-2012-2652), CONICET (PIP 11220130100075) and MINCYT-Córdoba (GRFT Res. 109/2017) for support. VM, MSB and DAG are CONICET Career Members. All calculations were performed with computational resources from CCAD - Universidad Nacional de Córdoba (<http://ccad.unc.edu.ar/>).

## Appendix A. Supplementary data

Supplementary data to this article can be found online at <https://doi.org/10.1016/j.bbamem.2018.05.012>.

## References

- [1] S.C. Lummis, GABA receptors in insects, *Comp. Biochem. Physiol. C, Comp. Pharmacol Toxicol.* 95 (1990) 1–8.
- [2] E. Sigel, M.E. Steinmann, Structure, function, and modulation of GABA(A) receptors, *J. Biol. Chem.* 287 (2012) 40224–40231.
- [3] L. Chen, L. Xue, K.M. Giacomini, J.E. Casida, GABAA receptor open-state conformation determines non-competitive antagonist binding, *Toxicol. Appl. Pharmacol.* 250 (2011) 221–228.
- [4] P. Kumar, S. Mishra, A. Malik, S. Satya, Insecticidal properties of *Mentha* species: a review, *Ind. Crop. Prod.* 34 (2011) 802–817.
- [5] M. Sanchez-Borzone, L. Delgado-Marin, D.A. Garcia, Inhibitory effects of carvone isomers on the GABAA receptor in primary cultures of rat cortical neurons, *Chirality* 26 (2014) 368–372.
- [6] M.E. Sanchez-Borzone, L.D. Marin, D.A. Garcia, Effects of insecticidal ketones present in mint plants on GABAA receptor from mammalian neurons, *Pharmacogn. Mag.* 13 (2017) 114–117.
- [7] K.M. Hold, N.S. Sirisoma, T. Ikeda, T. Narahashi, J.E. Casida, Alpha-thujone (the active component of absinthe): gamma-aminobutyric acid type A receptor modulation and metabolic detoxification, *Proc. Natl. Acad. Sci. U. S. A.* 97 (2000) 3826–3831.
- [8] M.M. Czyzewska, J.W. Mozrzyms, Monoterpene alpha-thujone exerts a differential inhibitory action on GABA(A) receptors implicated in phasic and tonic GABAergic inhibition, *Eur. J. Pharmacol.* 702 (2013) 38–43.
- [9] D.A. Garcia, M.A. Perillo, Localization of flunitrazepam in artificial membranes. A spectrophotometric study about the effect the polarity of the medium exerts on flunitrazepam acid-base equilibrium, *Biochim. Biophys. Acta* 1324 (1997) 76–84.
- [10] D.A. Garcia, M.A. Perillo, Partitioning of flunitrazepam into model membranes studied by temperature controlled gel filtration chromatography, *Biomed. Chromatogr.* 11 (1997) 343–347.
- [11] M.E. Mariani, M.E. Sanchez-Borzone, D.A. Garcia, Effects of bioactive monoterpene ketones on membrane organization. A Langmuir film study, *Chem. Phys. Lipids* 198 (2016) 39–45.
- [12] G.N. Reiner, L.F. Fraceto, E.D. Paula, M.A. Perillo, D.A. García, Effects of GABAergic phenols on phospholipid bilayers as evaluated by <sup>1</sup>H-NMR, *J. Biomater. Nanobiotechnol.* 04 (2013) 28–34.
- [13] G.N. Reiner, D.O. Labuckas, D.A. Garcia, Lipophilicity of some GABAergic phenols and related compounds determined by HPLC and partition coefficients in different systems, *J. Pharm. Biomed. Anal.* 49 (2009) 686–691.
- [14] G.N. Reiner, M.A. Perillo, D.A. Garcia, Effects of propofol and other GABAergic phenols on membrane molecular organization, *Colloids Surf. B Biointerfaces* 101 (2013) 61–67.
- [15] R. Sogaard, T.M. Werge, C. Bertelsen, C. Lundbye, K.L. Madsen, C.H. Nielsen, J.A. Lundbaek, GABA(A) receptor function is regulated by lipid bilayer elasticity, *Biochemistry* 45 (2006) 13118–13129.
- [16] T.W. Sirk, E.F. Brown, M. Friedman, A.K. Sum, Molecular binding of catechins to biomembranes: relationship to biological activity, *J. Agric. Food Chem.* 57 (2009) 6720–6728.
- [17] J.L. Lopes, N.F. Valadares, D.I. Moraes, J.C. Rosa, H.S. Araujo, L.M. Beltramini, Physico-chemical and antifungal properties of protease inhibitors from *Acacia plumosa*, *Phytochemistry* 70 (2009) 871–879.
- [18] R.S. Cantor, The lateral pressure profile in membranes: a physical mechanism of general anesthesia, *Biochemistry* 36 (1997) 2339–2344.
- [19] B. Hess, C. Kutzner, D. van der Spoel, E. Lindahl, GROMACS 4: algorithms for highly efficient, load-balanced, and scalable molecular simulation, *J. Chem. Theory Comput.* 4 (2008) 435–447.
- [20] J.P. Jambeck, A.P. Lyubartsev, Derivation and systematic validation of a refined all-atom force field for phosphatidylcholine lipids, *J. Phys. Chem. B* 116 (2012) 3164–3179.
- [21] W.L. Jorgensen, J. Chandrasekhar, J.D. Madura, R.W. Impey, M.L. Klein, Comparison of simple potential functions for simulating liquid water, *J. Chem. Phys.* 79 (1983) 926.
- [22] V. Miguel, M.E. Defonsi Lestard, M.E. Tuttolomondo, S.B. Diaz, A.B. Altabef, M. Puiatti, A.B. Pierini, Molecular view of the interaction of S-methyl methanethiosulfonate with DPPC bilayer, *Biochim. Biophys. Acta* 1858 (2016) 38–46.
- [23] M.E. Sanchez-Borzone, M.E. Mariani, V. Miguel, R.M. Gleiser, B. Odhav, K.N. Venugopala, D.A. Garcia, Membrane effects of dihydropyrimidine analogues with larvicidal activity, *Colloids Surf. B Biointerfaces* 150 (2017) 106–113.
- [24] J. Wang, R.M. Wolf, J.W. Caldwell, P.A. Kollman, D.A. Case, Development and testing of a general amber force field, *J. Comput. Chem.* 25 (2004) 1157–1174.
- [25] J. Wang, P. Cieplak, P.A. Kollman, How well does a restrained electrostatic potential (RESP) model perform in calculating conformational energies of organic and biological molecules? *J. Comput. Chem.* 21 (2000) 1049–1074.
- [26] C.I. Bayly, P. Cieplak, W. Cornell, P.A. Kollman, A well-behaved electrostatic potential based method using charge restraints for deriving atomic charges: the RESP model, *J. Phys. Chem.* 97 (1993) 10269–10280.
- [27] M.J. Frisch, G.W. Trucks, H.B. Schlegel, G.E. Scuseria, M.A. Robb, J.R. Cheeseman, J.A. Montgomery Jr., T. Vreven, K.N. Kudin, J.C. Burant, J.M. Millam, S.S. Iyengar, J. Tomasi, V. Barone, B. Mennucci, M. Cossi, G. Scalmani, N. Rega, G.A. Petersson, H. Nakatsuji, M. Hada, M. Ehara, K. Toyota, R. Fukuda, J. Hasegawa, M. Ishida, T. Nakajima, Y. Honda, O. Kitao, H. Nakai, M. Klene, X. Li, J.E. Knox, H.P. Hratchian, J.B. Cross, V. Bakken, C. Adamo, J. Jaramillo, R. Gomperts, R.E. Stratmann, O. Yazyev, A.J. Austin, R. Cammi, C. Pomelli, J.W. Ochterski, P.Y. Ayala, K. Morokuma, G.A. Voth, P. Salvador, J.J. Dannenberg, V.G. Zakrzewski, S. Dapprich, A.D. Daniels, M.C. Strain, O. Farkas, D.K. Malick, A.D. Rabuck, K. Raghavachari, J.B. Foresman, J.V. Ortiz, Q. Cui, A.G. Baboul, S. Clifford, J. Cioslowski, B.B. Stefanov, G. Liu, A. Liashenko, P. Piskorz, I. Komaromi, R.L. Martin, D.J. Fox, T. Keith, M.A. Al-Laham, C.Y. Peng, A. Nanayakkara, M. Challacombe, P.M.W. Gill, B. Johnson, W. Chen, M.W. Wong, C. Gonzalez, J.A. Pople, Gaussian 03, Revision C.02, Gaussian, Inc., Wallingford, CT, 2004.
- [28] A.W. Sousa Da Silva, W.F. Vranken, ACPYPE - AnteChamber PYthon Parser interface, *BMC Res. Notes* 5 (2012) 367.
- [29] S. Kumar, J.M. Rosenberg, D. Bouzida, R.H. Swendsen, P.A. Kollman, The weighted histogram analysis method for free-energy calculations on biomolecules. I. The method, *J. Comput. Chem.* 13 (1992) 1011–1021.
- [30] J.S. Hub, B.L. de Groot, D. van der Spoel, g\_wham—a free weighted histogram analysis implementation including robust error and autocorrelation estimates, *J. Chem. Theory Comput.* 6 (2010) 3713–3720.
- [31] U. Essmann, L. Perera, M.L. Berkowitz, T. Darden, H. Lee, L.G. Pedersen, A smooth particle mesh Ewald method, *J. Chem. Phys.* 103 (1995) 8577.
- [32] A.D. Bangham, M.W. Hill, N.G.A. Miller, Preparation and Use of Liposomes as Models of Biological Membranes, (1974), pp. 1–68.
- [33] W. Kopec, J. Telenius, H. Khandelia, Molecular dynamics simulations of the interactions of medicinal plant extracts and drugs with lipid bilayer membranes, *FEBS J.* 280 (2013) 2785–2805.
- [34] A. Seelig, J. Seelig, The dynamic structure of fatty acyl chains in a phospholipid bilayer measured by deuterium magnetic resonance, *Biochemistry* 13 (1974) 4839–4845.
- [35] P.L. Yeagle, *The Structure of Biological Membranes*, third ed., Ergodebooks, 2011.
- [36] A. Botan, F. Favela-Rosales, P.F. Fuchs, M. Javanainen, M. Kanduc, W. Kulig, A. Lamberg, C. Loison, A. Lyubartsev, M.S. Miettinen, L. Monticelli, J. Maatta, O.H. Ollila, M. Retegan, T. Rog, H. Santuz, J. Tynkynen, Toward atomistic resolution structure of phosphatidylcholine headgroup and glycerol backbone at different ambient conditions, *J. Phys. Chem. B* 119 (2015) 15075–15088.
- [37] S. Jakobtorweihen, A.C. Zuniga, T. Ingram, T. Gerlach, F.J. Keil, I. Smirnova, Predicting solute partitioning in lipid bilayers: free energies and partition coefficients from molecular dynamics simulations and COSMOmic, *J. Chem. Phys.* 141 (2014) 045102.
- [38] M. Ahumada, C. Calderón, A. Lissie, Temperature dependence of bilayer properties in liposomes and the use of fluorescent probes as a tool to elucidate the permeation mechanism of hydrophilic solutes, *J. Chil. Chem. Soc.* 61 (2016) 3052–3054.
- [39] R.L. Biltonen, D. Lichtenberg, The use of differential scanning calorimetry as a tool to characterize liposome preparations, *Chem. Phys. Lipids* 64 (1993) 129–142.
- [40] Z.V. Leonenko, E. Finot, H. Ma, T.E.S. Dahms, D.T. Cramb, Investigation of temperature-induced phase transitions in DOPC and DPPC phospholipid bilayers using temperature-controlled scanning force microscopy, *Biophys. J.* 86 (2004) 3783–3793.
- [41] F.G. Prendergast, R.P. Haugland, P.J. Callahan, 1-[4-(Trimethylamino)phenyl]-6-phenylhexa-1,3,5-triene: synthesis, fluorescence properties and use as a fluorescence probe of lipid bilayers, *Biochemistry* 20 (1981) 7333–7338.
- [42] A. do Canto, J.R. Robalo, P.D. Santos, A.J.P. Carvalho, J.P.P. Ramalho, L.M.S. Loura, Diphenylhexatriene membrane probes DPH and TMA-DPH: a comparative molecular dynamics simulation study, *Biochim. Biophys. Acta* 1858 (2016) 2647–2661.
- [43] R. Pavela, History, presence and perspective of using plant extracts as commercial botanical insecticides and farm products for protection against insects—a review, *Plant Protect. Sci.* 52 (2016) 229–241.
- [44] J.M. Herrera, M.P. Zunino, J.S. Dambolena, R.P. Pizzolitto, N.A. Gañan, E.I. Lucini, J.A. Zygadlo, Terpene ketones as natural insecticides against *Sitophilus zeamais*, *Ind. Crop. Prod.* 70 (2015) 435–442.

- [45] O.H. Samuli Ollila, T. Rog, M. Karttunen, I. Vattulainen, Role of sterol type on lateral pressure profiles of lipid membranes affecting membrane protein functionality: comparison between cholesterol, desmosterol, 7-dehydrocholesterol and ketosterol, *J. Struct. Biol.* 159 (2007) 311–323.
- [46] T. Rog, L.M. Stimson, M. Pasenkiewicz-Gierula, I. Vattulainen, M. Karttunen, Replacing the cholesterol hydroxyl group with the ketone group facilitates sterol flip-flop and promotes membrane fluidity, *J. Phys. Chem. B* 112 (2008) 1946–1952.
- [47] S. Witzke, L. Duelund, J. Kongsted, M. Petersen, O.G. Mouritsen, H. Khandelia, Inclusion of terpenoid plant extracts in lipid bilayers investigated by molecular dynamics simulations, *J. Phys. Chem. B* 114 (2010) 15825–15831.
- [48] Q.D. Pham, D. Topgaard, E. Sparr, Cyclic and linear monoterpenes in phospholipid membranes: phase behavior, bilayer structure, and molecular dynamics, *Langmuir ACS J. Surf. Colloids* 31 (2015) 11067–11077.